Pathogenic Keratinocyte States and Fibroblast Niches Define the Tissue Microenvironment in Severe Hidradenitis Suppurativa

Xinyi Du-Harpur*[1,2,3], Clarisse Ganier*[1,4], Pavel Mazin[5], Chris Cheshire[2], Ellie Rashidghamat[6], Nicholas M. Luscombe[2,7], Magnus D. Lynch[1,6], Fiona M. Watt[1,8]

These authors contributed equally to this work.

Affiliations:

1. Centre for Gene Therapy and Regenerative Medicine, King's College London, Great Maze Pond, London SE1 9RT, United Kingdom
2. The Francis Crick Institute, 1 Midland Road, London NW1 1AT, United Kingdom
3. St John's Institute of Dermatology, King's College London, Great Maze Pond, London SE1 9RT, United Kingdom
4. Meta-Organism Unit, Institut Pasteur, 25-28 Rue du Dr Roux, 75015 Paris, France
5. Wellcome Sanger Institute, Wellcome Genome Campus, Hinxton, Cambridge, CB10 1RQ
6. St John's Institute of Dermatology, Guys and St Thomas' NHS Foundation Trust, Great Maze Pond, London SE1 9RT, United Kingdom

7. Okinawa Institute of Science and Technology Graduate University, 1919-1 Tancha, Onnason, Okinawa 904-0495, Japan.
8. The Directors' Research Unit, European Molecular Biology Laboratory, Meyerhofstrasse 1, 69117 Heidelberg, Germany

Correspondence:

Xinyi Du-Harpur, St. John's Institute of Dermatology, King's College London, Great Maze Pond London SE1 9RT, United Kingdom. E-mail: xinyi.duharpur@kcl.ac.uk; **Clarisse Ganier,** Meta-organism Unit, Immunology Department, Institut Pasteur, 25-28 Rue du Dr Roux, 75015 Paris, France. E-mail: clarisse.ganier@pasteur.fr; and **Fiona M. Watt,** The Directors' Research Unit, European Molecular Biology Laboratory, Meyerhofstrasse 1, Heidelberg 69117, Germany. E-mail: fiona.watt@embo.org

ABSTRACT

Hidradenitis suppurativa (HS) is a chronic inflammatory skin disease characterized by recurrent painful abscesses and tunnels in flexural sites. The mechanisms driving HS pathogenesis, particularly the roles of keratinocytes and fibroblasts in the HS inflammatory ecosystem, remain poorly understood. To characterise the cellular and molecular landscape of HS, we analyzed lesional skin from severe HS patients using single-cell RNA-sequencing and spatial transcriptomics to identify key keratinocyte states and cellular interactions, with a focus on fibroblast–keratinocyte crosstalk. Our study identifies a novel migratory S100+ pathogenic keratinocyte state and highlights critical interactions between COL6A5+ fibroblasts in HS lesion formation. We also detect tertiary lymphoid organ (TLO)-like structures enriched with activated B and plasma cells interacting with APOD+ fibroblasts, implicating their role in HS chronic inflammation. We show that fibroblast interactions with HS keratinocytes and specific immune cells, such as Langerhans cells, are key drivers of HS pathogenesis, and that two main fibroblast niches are present within the HS microenvironment. Targeting these cellular networks may offer new therapeutic strategies for HS management, and highlight the potential limitations of targeting individual pathways in isolation, when treating pathology present in HS tissue.

MAIN TEXT

Introduction

Hidradenitis suppurativa (HS) is a chronic inflammatory skin disease that affects approximately 1% of individuals in western countries (Ingram 2020). It is characterised by the formation of painful nodules, abscesses and tunnels in flexural sites such as axillae and groin, leading to considerable psychosocial morbidity and impact on daily activities (Nguyen et al. 2021). HS is also associated with significantly increased cardiovascular adverse events, increased cancer risk and reduced life expectancy (Tiri et al. 2019).

HS pathogenesis originates in the pilosebaceous unit, where altered epidermal keratinisation, dysregulated innate immunity and dysbiosis leads to comedogenesis and inflammation (Frew 2020). Severe HS (Hurley stage III) is characterised by the formation of tunnels, whereby keratinocytes invade the dermis and form structures that generate inflammatory exudate and propagate inflammation (Navrazhina et al. 2021). Dysbiosis, specifically an increased abundance of anaerobes such as *Prevotella*, is a feature of HS, with perilesional tissue demonstrating microbiome shifts reminiscent of lesional tissue (Riverain-Gillet et al. 2020).

Increased inflammation from immune signaling is observed in HS, with recent transcriptomic studies focusing on the role of polarised macrophages, B cells and tertiary lymphoid organs (TLOs) (Gudjonsson et al. 2020; Lowe et al. 2024; Mariottoni et al. 2021; Yu et al. 2024), which represent ectopic germinal center-like aggregates of immune cells and can arise in the context of chronic inflammation

(Dong et al. 2023). Recently approved therapeutic options for severe HS are based on inhibition of IL-17 and TNF-alpha, and there are also promising clinical investigations into targeting JAK/STAT signalling (Krueger et al. 2024). However, those treatment options are often only partially effective.

Over the past two decades, studies characterising the genetic architecture of HS have repeatedly identified epidermal differentiation as a key pathogenic factor in HS. Research into monogenic HS has highlighted the important role of γ-secretase in disease onset. γ-secretase in an intramembranous protease complex, which can cleave numerous transmembrane proteins including Notch receptors and cadherin (Pink et al. 2013). In mouse models, alterations in γ-secretase function lead to follicular keratinisation, epidermal cysts, epidermal hyperplasia and lack of sebaceous glands (Pan et al. 2004). A recent genome-wide association meta-analysis has confirmed the importance of both Notch and Wnt/β-catenin signaling pathways as being key to HS pathogenesis (Kjærsgaard Andersen et al. 2025). A previous GWAS identified SOX9 and KLF5 as putative causal genes in HS (Sun et al. 2023). SOX9 is a pioneer transcription factor that regulates fate determination of hair follicle outer root sheath keratinocytes (Yang et al. 2023). Hyperplasia of the outer root sheath is the characteristic histological feature of the very earliest stages of HS (Dunstan et al. 2021), and is observed clinically as comedone formation.

In light with those findings, we used single-cell RNA sequencing (scRNAseq) and spatial transcriptomics (ST) to dissect the HS transcriptomic landscape, focusing on epidermal differentiation. We have identified HS-specific pathogenic keratinocyte states, and the importance of specific fibroblast subpopulations in driving the

inflammatory ecosystem in HS. These findings suggest new therapeutic strategies that can be used in combination with current approaches to tackle the high healthcare burden of HS (Garg et al. 2020).

Results

Characterisation of cellular heterogeneity in lesional HS tissue

ScRNAseq (3') data was generated from lesional axillary skin of 3 donors with severe HS (Figure 1A, Supplementary Figure 1A-B). Cell type annotation of scRNAseq data was performed following clustering and analysis of differentially expressed genes using Seurat. This identified 7 keratinocyte clusters, 3 fibroblast clusters as well as melanocytes, pericytes, endothelial cells (vascular and lymphatic) and multiple immune cell clusters including langerhans cells, macrophages, mast cells, B and plasma cells (Figure 1B, C).

Transcriptional and spatial identification of a novel HS migratory S100+ Keratinocyte state

Keratinocyte clusters were annotated according to their mean expression of gene signature modules representing functional characteristics (Table 1). The 7 keratinocyte clusters identified were further characterized with proliferative, basal, differentiated, hair, sweat and sebaceous scores (Figure 1D). HS specific gene signature modules included HS tunnel, inflammatory, migratory and stress response genes. We were also able to identify a keratinocyte state characterised by high

expression of proliferation, differentiation, migration, inflammation and stress response genes. This cell state simultaneously showed high expression of sebocyte and HS tunnel genes, consistent with recently published work suggesting the cell of origin is infundibular (Yu et al. 2024). We characterised this cluster as a pathogenic HS keratinocyte state, with representative marker genes including S100A7, S100A8, S100A9 and S100A12 (Figure 1E), in keeping with previous work by Jin et al (Jin et al. 2023).

Lineage trajectory and pseudotime analysis using Monocle (Figure 1F, 1G) showed that basal keratinocytes are predicted to progress through dividing, spinous and migratory transitional keratinocyte (K) states prior to differentiating into three differentiated states: immunobarrier K, migratory S100+ K and hair / sweat glandular K. A transitional remodeling K cluster was observed within a closed loop trajectory, which could imply a dedifferentiation phenomenon and high tissue plasticity in HS keratinocytes, a mechanism demonstrated in GATA6+ keratinocytes in mouse adult wounded epidermis (Bernabé-Rubio et al. 2023).

Having catalogued keratinocytes populations from HS lesional tissues, we localised them within the tissue using 10X Visium global spatial transcriptomics (ST). To clarify the spatial distribution of the different cell types identified in our scRNAseq dataset, we used a cell2location algorithmic approach to spatially predict the annotated scRNAseq clusters onto ST (Visium).

We prepared ST libraries for 4 HS skin samples. The Unique Molecular Identifier (UMI) counts per spot, number of genes per spot and the percentage of

mitochondrial genes in all the HS sections used for the 10X Visium protocol confirmed that the libraries were of high quality (Supplementary Figure 1C-D), and the few low quality spots were removed. To deconvolve cell types present within each Visium 55µm grid spot, we used a previously published algorithm, cell2location (Kleshchevnikov et al. 2022), a Bayesian model that can resolve fine-grained cell types in ST data to create comprehensive cellular maps of diverse tissues, permitting the inference of cell types present based on an annotated scRNAseq dataset.

Cell2location analysis showed that dividing K were sporadically distributed in the epidermis and HS tunnels (identified by H&E). Basal K were identified in the basal layer of both the interfollicular epidermis and in HS tunnels, and basal/spinous K showed a similar pattern but in between basal and spinous layers of the interfollicular epidermis and HS tunnels. Interestingly, transitional remodeling K were deconvoluted throughout the interfollicular epidermis layers except for the granular layer; with the same pattern being demonstrated within HS tunnels. Immunobarrier K were spatially consistent with the most differentiated and granular layer of the interfollicular epidermis, and the innermost layer of the HS tunnel. Hair and sweat glandular keratinocytes were specifically located in the sweat gland regions and in hair follicles of healthy samples (Supplementary Figure 2A), and could implicate residual hair follicles in HS sections. Critically, these were not located in HS tunnels. Finally, migratory S100+ K / sebocytes were located in specific regions of HS tunnels in our samples, and were found within the sebocytes of healthy samples (Figure 2, Supplementary Figure 2A).

Fibroblast–Keratinocyte Crosstalk Dominates the Cellular Interaction Landscape in Severe HS Lesions

Next, we performed cell-cell interaction analysis on scRNAseq data using CellChat to understand which cellular interactions were driving HS keratinocyte states. CellChat identified fibroblast-keratinocyte interactions to be the strongest (Figure 3A) and most numerous (Figure 3B) interactions. In particular, SFRP4+ reticular fibroblasts and COL6A5+ papillary fibroblasts had the highest outgoing communication score, and transitional remodeling keratinocytes, basal keratinocytes and migratory S100+ keratinocytes demonstrated the highest incoming interaction strength (Fig 3C). Collagen, laminin and desmosomes were found to be the top 3 signalling pathways in HS tissue (Figure 3D).

Communication patterns within scRNAseq data were also analysed using CellChat, which provides insights into how cell types and signaling pathways are coordinated (Figure 3E). CellChat performs this analysis by using a pattern recognition method based upon non-negative matrix factorization, enabling identification of global communication patterns as well as the important signals within different cell groups. By applying this analysis, we were able to identify 2 distinct signalling patterns arising from fibroblasts: COL6A5+ papillary fibroblasts were identified as having their own communication pattern (Pattern 5), responsible for pathways such as non-canonical Wnt signalling and activin, which is part of the TGF-β superfamily. These pathways are implicated in processes such as epithelial migration, invasion and epithelial-mesenchymal transition (EMT) (Bashir et al. 2015; Liu et al. 2022; Weiss and Attisano 2013). In contrast, SFRP4+ and APOD+ fibroblasts share a signaling

pattern (pattern 2) responsible for pathways such as collagen, fibronectin, FGF and IGF.

To spatially complement this analysis, we then used Pearson correlation coefficients (PCC) of spot normalized cell abundances from the cell2location predictions in all the ST samples to quantitatively analyse the co-localisation of cell subpopulations in HS lesional skin, as an orthogonal approach to validate predicted cellular interactions (Figure 4A, 4B, 4C). We found that the main fibroblast subpopulation interacting with HS keratinocytes was COL6A5+ papillary fibroblasts, which were shown to co-localise most strongly with undifferentiated HS keratinocytes, specifically the basal and dividing keratinocyte subpopulations. In contrast, APOD+ inflammatory fibroblasts co-localised with hair/sweat gland keratinocyte subpopulations. Furthermore, SFRP4+ reticular fibroblasts did not directly co-localise with keratinocytes, as expected for a reticular-like signature, but interestingly did co-localise with immune cells such as macrophages and mast cells (Figure 4D). Altogether, these findings highlight COL6A5+ papillary fibroblasts as the main contributors to the fibroblast–keratinocyte communication network in HS.

APOD+ fibroblasts support TLO-like structures and its associated immune niches localize within HS Lesions

TLOs have recently been proposed to play an important role in HS pathogenesis (Gudjonsson et al. 2020; Lowe et al. 2024; Yu et al. 2024). A key feature of TLOs is clonal expansion of plasma cells and proliferating B cells. In our analysis, plasma/B cells were relatively abundant and are over-represented in HS compared to other

inflammatory skin diseases (Supplementary Figure 2B). Further analysis of these subpopulations identified an activated B cell phenotype with increased expression of AICDA, amongst other genes (Figure 5A-B) (Horns et al. 2020). AICDA is responsible for somatic hypermutation and class-switch recombination, typically facilitating antibody diversification in secondary lymphoid tissues (Honjo et al. 2002). The spatial localisation of this activated B cell phenotype adjacent to follicular HS structures was further characterised with immunofluorescence using the markers CD20, Tbx21 and CD11c, which are recognised markers of B cell activation and have been used to characterise TLOs (Figure 5C) (Rubtsova et al. 2017; Sato et al. 2023). Plasma and B cells were mapped onto HS Visium slides using cell2location (Figure 5D) as well as through the plotting of plasma cell markers (IGHA1, IGHM, IGHG1) which demonstrated abundance of plasma / B cells surrounding pathogenic HS structure, and in particular high expression of IgA and IgG immunoglobulins in ST (Figure 5E), correlated with the similar level of expression of IgA and IgG by plasma cells in scRNAseq (Figure 5F).

We utilised PCC to characterise the cell types co-localising with B and plasma cells. In our analysis, plasma and B cells showed strongest colocalisation with APOD+ fibroblasts and dendritic cells, and to a lesser extent mast cells and T cells (Figure 5G). Further analysis showed that APOD+ inflammatory fibroblasts were found to co-localise with vascular endothelial cells and pericytes (Figure 5H). In scRNAseq data, endothelial cells in HS were found to have high expression of ACKR1, a marker of venular endothelial cells which encodes a membrane protein that supports immune cell trafficking also seen in other inflammatory skin diseases (Reynolds et al. 2021). In lesional HS, the expression of ACKR1 was proportionally greater than that

observed in endothelial cells in lesional eczema and psoriasis (Supplementary Figure 2C). These findings support the concept of TLOs being present in HS lesional tissue and suggest APOD+ inflammatory fibroblasts as playing a critical role within these structures.

Next, we explored the signaling interactions within TLOs. CellChat analysis showed that Langerhans cells, T cells, dendritic cells, macrophages, B cells and mast cells coordinate the most expansive communication pattern (Pattern 3) that includes typical HS cytokine signatures such as TNF, IL-1 and TGF-β (Figure 3E). Interestingly, plasma/B cells did not show high interaction strength either as senders or receivers (Figure 3C) in scRNAseq cell-cell interaction analysis, and plasma cells are absent in cell communication analysis (Figure 3E). This suggests that they are unlikely to alter HS keratinocytes through direct cellular interactions, but may amplify inflammation indirectly through the production of antibodies.

Recently, Langerhans cells have been identified as being critical coordinators of TLO formation in mouse skin, in response to colonising micro-organisms (Gribonika et al. 2025). In our data, we identified Langerhans cells as being the immune cell type with the highest ‘incoming interaction’ score. Furthermore, Langerhans cells were predicted to co-localise with COL6A5+ papillary fibroblasts as well as pathogenic HS keratinocytes (Figure 5I). This suggests that Langerhans cells may function as a critical relay point between keratinocytes forming pathogenic HS lesions, and the TLOs sustaining inflammation to promote their formation.

Overall, our findings suggest that there are two distinct and important fibroblast niches; COL6A5+ fibroblasts enable the development of pathogenic HS keratinocytes, whilst APOD+ fibroblasts form the architecture to recruitment and development of cell types necessary to support chronic inflammatory HS lesions.

Discussion:

The genetic architecture of HS consistently implicates epidermal differentiation in its pathophysiology (Kjærsgaard Andersen et al. 2025). Recent work by Navrazhina et al. and Jin et al. has placed keratinocytes at the centre of HS pathogenesis (Jin et al. 2023; Navrazhina et al. 2021). Navrazhina et al. identified tunnel epithelium as being chemotactic and pro-inflammatory, whilst Jin et al. identified a HS keratinocyte state, which arises due to basal keratinocytes becoming epigenetically reprogrammed towards a hyperproliferative and pro-inflammatory state in HS (Jin et al. 2023).

Although pro-fibrotic and pro-inflammatory HS fibroblast subpopulations have previously been described in HS (van Straalen et al. 2024), the interaction and co-localisation of fibroblast populations with pathogenic HS keratinocytes have not been previously well understood. In HS, keratinocytes breach their physiological compartment and invade the dermis, forming 3-dimensional structures representing inflammatory epithelial niches. Our work showed that COL6A5+ papillary fibroblasts, which co-localise and signal to basal keratinocytes, promote the migratory and proliferative pathogenic cell state critical to HS pathogenesis. This interaction mirrors the developmental origin of skin appendages such as pilosebaceous units, since papillary fibroblasts are necessary for formation of these structures (Driskell et al. 2013; Philippeos et al. 2018). Ultimately, the formation of epithelial structures seen in

severe HS requires remodelling of the connective tissue to support their physical advancement and progression into the dermis. We also characterised a second fibroblast niche dominated by APOD+ fibroblasts, that co-localise with pericytes, endothelial cells, plasma cells and B cells. These suggest that in severe HS, the APOD+ fibroblast niche supports the immune and stromal cells that aggregate in the formation of TLOs, which are increasingly recognised to promote and sustain inflammation in the HS tissue microenvironment.

Abnormal keratinisation and barrier alteration are recognised as a key factor in the development of HS (Frew 2020; Zouboulis et al. 2020). Epithelial barrier function influences skin microbial communities and how it activates the innate immune system (Belkaid and Tamoutounour 2016). The skin microbiome's role in HS pathogenesis is implicated by, firstly, the efficacy of antibiotics in suppressing HS inflammation and their continued use as first-line HS therapy (Sabat et al. 2020). Secondly, the HS microbiome shifts are first seen in non-lesional HS tissue and become more marked as HS progresses (Ring et al. 2017). Recent work has also shown that the gram-negative anaerobes that dominate the HS microbiome directly activate keratinocytes (Williams et al. 2024), giving some mechanistic validation to the hypothesis that the skin microbiome may precede clinically apparent HS. Interestingly, in our data, Langerhans cells, which survey the skin barrier for harmful microbes, occupy the COL6A5+ fibroblast niche which we defined as initiating HS lesions. Langerhans cells have recently been identified as a key cell type expressing genes related to the NLRP3 inflammasome (Moran et al. 2023), which are strongly implicated in HS pathogenesis (Johnston et al. 2021) and are also recognised to coordinate bacteria-induced TLO formation (Gribonika et al. 2025).

Current therapeutic strategies in HS are based upon targeting immune pathways, such as TNF-alpha and IL-17. However, there remains widespread dissatisfaction with treatments currently available for HS (Garg et al. 2020). Treatments are often only partially effective, and primary or secondary failures are seen relatively frequently in HS (Aarts et al. 2021). Our data demonstrates the presence of two distinct fibroblast niches within the HS tissue microenvironment, reflecting distinct cellular networks driving aspects of HS pathogenesis. This is unlikely to be addressed by the targeting of an individual pathway. We propose that future treatment strategies will need to address both the primary dysfunction occurring at the epithelial barrier, where innate immune cells and keratinocytes are activated, and the chronic inflammatory response that can subsequently arise within HS skin.

Materials and Methods:

Patients and samples:

Lesional HS skin from 3 donors was obtained from wide local excision surgery following ethical approval (REC reference 19/NE/0063). Patients provided written informed consent prior to surgery.

Generation of HS single-cell RNA-seq and spatial transcriptomic data

HS skin was enzymatically dissociated to separate epidermis and dermis, followed by preparation of single-cell suspensions using standard procedures. Cells were stained with a viability dye, sorted by FACS, and assessed for viability prior to loading on the 10x Genomics Chromium platform (Single Cell 3′). Libraries were

sequenced on an Illumina HiSeq 4000 and processed with CellRanger against GRCh38.

Fresh-frozen HS skin was embedded in OCT, cryo-sectioned, and processed on 10x Genomics Visium (Spatial 3′). RNA integrity was assessed using RNAscope with housekeeping control probes. Library quality was verified prior to sequencing on an Illumina HiSeq 4000. Reads were processed using spaceranger with GRCh38.

Further information regarding digestion conditions, instrument models, probe sets, fluorophores, and tissue optimization parameters are detailed in the *Supplementary Materials and Methods*.

ScRNAseq and spatial transcriptomic data analysis

scRNA-seq and spatial data underwent quality control, normalization, dimensionality reduction, and clustering in Seurat v5.1 (Hao et al. 2024). Cell types were assigned by canonical marker genes and gene ontology of cluster-enriched features. Datasets were integrated using Harmony (Korsunsky et al. 2019) for downstream analyses.

Cell type abundances across Visium spots were inferred using cell2location trained on the scRNA-seq reference. To identify tissue microenvironments characterized by co-occurring cell types, we applied non-negative matrix factorization (NMF) to normalized cell type abundance estimates across Visium spots. Further details regarding cell2location and colocalisation analysis are described in the *Supplementary Materials and Methods*.

Keratinocyte lineage dynamics were analyzed with Monocle 3 (Cao et al. 2019). Cells were converted from Seurat to Monocle, partitioned, and ordered in pseudotime with the basal keratinocyte population set as the root state. Ligand–receptor-mediated signaling between cell states was inferred using CellChat (Jin et

al. 2025) on the annotated scRNA-seq dataset. We computed communication probabilities and performed pathway-level input/output analyses using the standard pipeline.

Immunohistochemistry and microscopy

Skin samples were embedded in OCT and cryo-sectioned at 10–16 µm thickness. Sections were fixed in 4% paraformaldehyde, blocked in serum-based buffer, and incubated with primary antibodies overnight at 4 °C. After washing, sections were labeled with secondary antibodies and DAPI, then mounted with antifade medium. Full reagent details, concentrations, incubation times, and microscopy analysis details are provided in *Supplementary Materials and Methods*.

Ethics statement:

The study was sponsored by Guy's and St Thomas' NHS Foundation Trust and King's College London and was subject to both institutional and external research ethics council (REC) review (REC reference 19/NE/0063).

Data Availability Statement:

The raw and processed datasets for scRNAseq and Visium ST generated in the current study are available on ArrayExpress.

ORCIDs:

Xinyi Du-Harpur: https://orcid.org/0000-0002-5738-8734

Clarisse Ganier: https://orcid.org/0000-0003-1143-7905

Pavel Mazin: https://orcid.org/0000-0001-9268-3352

Ellie Rashidghamat: https://orcid.org/0000-0002-1548-5528

Chris Cheshire: https://orcid.org/0000-0002-5806-2883

Nicholas M. Luscombe: https://orcid.org/0000-0001-5293-4778

Magnus D. Lynch: https://orcid.org/0000-0001-7586-4338

Fiona M. Watt: https://orcid.org/0000-0001-9151-5154

Conflict of Interest Statement:

XDH has received honoraria from AbbVie; served in advisory roles for RoC Skincare, Dermatica Ltd; and undertaken advisory and promotional roles for Simple Skincare, E45, Skin + Me Ltd., L'Oreal Dermatological Beauty and The Skin Diary Ltd. ER has served on advisory boards for Biogen, Novartis, and UCB; as investigator for trials sponsored by Boehringer Ingelheim, Novartis, Incyte, UCB, and Abbvie; received research funding from UCB; serves as medical director of Klira Ltd; and has undertaken promotional work for CeraVe, La Roche Posay, Eucerin, Paula's Choice, E45, Roc, and Garnier. MDL and FMW are co-founders of Fibrodyne Ltd, a company working on fibroblast cell therapies.

Acknowledgements:

XDH was the recipient of an Accelerator Award from Cancer Research United Kingdom, which supported this work. FMW acknowledges financial support from the United Kingdom Medical Research Council (MR/ PO18823/1), Biotechnology and Biological Sciences Research Council (BB/M007219/1), and the Wellcome Trust (206439/Z/17/Z) at the time of this work. This work was supported by the Francis Crick Institute, which receives its core funding from Cancer Research United Kingdom (FC010110), the United Kingdom Medical Research Council Journal of

Investigative Dermatology (FC010110), and the Wellcome Trust (FC010110). During this project, NML was a Winton Group leader in recognition of the Winton Charitable Foundation's support toward the establishment of the Francis Crick Institute. NML was also funded by a Wellcome Trust Joint Investigator Award (103760/Z/14/Z), the Medical Research Council eMedLab Medical Bioinformatics Infrastructure Award (MR/L016311/1), and received core funding from the Okinawa Institute of Science and Technology Graduate University. MDL gratefully acknowledges financial support from the Wellcome Trust (211276/E/18/Z).

The Advanced Sequencing Facility at the Francis Crick Institute provided protocols, technical support and guidance for single-cell RNA sequencing experiments. The Genome Centre, Queen Mary, University of London provided support with their genomics platform for spatial transcriptomics. Support for confocal microscopy was provided by King's College London Nikon Centre and Dr Ines Tomas.

Author Contribution Statement:

XDH: Conceptualization, Data Curation, Formal Analysis, Funding Acquisition, Investigation, Methodology, Project Administration, Visualization, Writing – original draft, Writing – review and editing

CG: Conceptualization, Formal Analysis, Investigation, Methodology, Project Administration, Visualization, Supervision, Writing – original draft, Writing – review and editing

PM: Data Curation, Software, Resources

CC: Data Curation, Resources

ER: Resources

NML: Conceptualization, Resources, Supervision, Writing – review & editing

MDL: Conceptualization, Methodology, Supervision, Visualization, Writing – review & editing

FMW: Conceptualization, Methodology, Resources, Supervision, Visualization, Writing – original draft, Writing – review & editing

References:

Aarts P, Dudink K, Vossen ARJV, van Straalen KR, Ardon CB, Prens EP, et al. Clinical Implementation of Biologics and Small Molecules in the Treatment of Hidradenitis Suppurativa. Drugs. 2021;81(12):1397–410

Bashir M, Damineni S, Mukherjee G, Kondaiah P. Activin-A signaling promotes epithelial-mesenchymal transition, invasion, and metastatic growth of breast cancer. NPJ Breast Cancer. Springer Science and Business Media LLC; 2015;1(1):15007

Belkaid Y, Tamoutounour S. The influence of skin microorganisms on cutaneous immunity. Nat. Rev. Immunol. 2016;16(6):353–66

Bernabé-Rubio M, Ali S, Bhosale PG, Goss G, Mobasseri SA, Tapia-Rojo R, et al. Myc-dependent dedifferentiation of Gata6+ epidermal cells resembles reversal of terminal differentiation. Nat. Cell Biol. Nat Cell Biol; 2023;25(10):1426–38

Cao J, Spielmann M, Qiu X, Huang X, Ibrahim DM, Hill AJ, et al. The single-cell transcriptional landscape of mammalian organogenesis. Nature. 2019;566(7745):496–502

Dong Y, Wang T, Wu H. Tertiary lymphoid structures in autoimmune diseases. Front. Immunol. 2023;14:1322035

Driskell RR, Lichtenberger BM, Hoste E, Kretzschmar K, Simons BD, Charalambous M, et al. Distinct fibroblast lineages determine dermal architecture in skin development and repair. Nature. 2013;504(7479):277–81

Dunstan RW, Salte KM, Todorović V, Lowe M, Wetter JB, Harms PW, et al. Histologic progression of acne inversa/hidradenitis suppurativa: Implications for future investigations and therapeutic intervention. Exp. Dermatol. 2021;30(6):820–30

Frew JW. Hidradenitis suppurativa is an autoinflammatory keratinization disease: A review of the clinical, histologic, and molecular evidence. JAAD Int. 2020;1(1):62–72

Garg A, Neuren E, Cha D, Kirby JS, Ingram JR, Jemec GBE, et al. Evaluating patients' unmet needs in hidradenitis suppurativa: Results from the Global Survey Of Impact and Healthcare Needs (VOICE) Project. J. Am. Acad. Dermatol. 2020;82(2):366–76

Gribonika I, Band VI, Chi L, Perez-Chaparro PJ, Link VM, Ansaldo E, et al. Skin autonomous antibody production regulates host-microbiota interactions. Nature. Nature; 2025;638(8052):1043–53

Gudjonsson JE, Tsoi LC, Ma F, Billi AC, van Straalen KR, Vossen ARJV, et al. Contribution of plasma cells and B cells to hidradenitis suppurativa pathogenesis. JCI Insight. 2020;5(19) Available from: http://dx.doi.org/10.1172/jci.insight.139930

Hao Y, Stuart T, Kowalski MH, Choudhary S, Hoffman P, Hartman A, et al. Dictionary learning for integrative, multimodal and scalable single-cell analysis. Nat. Biotechnol. Springer Science and Business Media LLC; 2024;42(2):293–304

Honjo T, Kinoshita K, Muramatsu M. Molecular mechanism of class switch recombination: linkage with somatic hypermutation. Annu. Rev. Immunol. 2002;20:165–96

Horns F, Dekker CL, Quake SR. Memory B Cell Activation, Broad Anti-influenza Antibodies, and Bystander Activation Revealed by Single-Cell Transcriptomics. Cell Rep. 2020;30(3):905–13.e6

Ingram JR. The epidemiology of hidradenitis suppurativa. Br. J. Dermatol. 2020;183(6):990–8

Jin L, Chen Y, Muzaffar S, Li C, Mier-Aguilar CA, Khan J, et al. Epigenetic switch reshapes epithelial progenitor cell signatures and drives inflammatory pathogenesis in hidradenitis suppurativa. Proc. Natl. Acad. Sci. U. S. A. Proc Natl Acad Sci U S A; 2023;120(49):e2315096120

Jin S, Plikus MV, Nie Q. CellChat for systematic analysis of cell-cell communication from single-cell transcriptomics. Nat. Protoc. Springer Science and Business Media LLC; 2025;20(1):180–219

Johnston DGW, Kirby B, Tobin DJ. Hidradenitis suppurativa: A folliculotropic disease of innate immune barrier dysfunction? Exp. Dermatol. 2021;30(10):1554–68

Kjærsgaard Andersen R, Stefansdottir L, Riis PT, Halldorsson G, Ferkingstad E, Oddsson A, et al. A genome-wide association meta-analysis links hidradenitis suppurativa to common and rare sequence variants causing disruption of the Notch and Wnt/β-catenin signaling pathways. J. Am. Acad. Dermatol. Elsevier BV; 2025;92(4):761–72

Kleshchevnikov V, Shmatko A, Dann E, Aivazidis A, King HW, Li T, et al. Cell2location maps fine-grained cell types in spatial transcriptomics. Nat. Biotechnol. Springer Science and Business Media LLC; 2022;40(5):661–71

Korsunsky I, Millard N, Fan J, Slowikowski K, Zhang F, Wei K, et al. Fast, sensitive and accurate integration of single-cell data with Harmony. Nat. Methods. Springer Science and Business Media LLC; 2019;16(12):1289–96

Krueger JG, Frew J, Jemec GBE, Kimball AB, Kirby B, Bechara FG, et al. Hidradenitis suppurativa: new insights into disease mechanisms and an evolving treatment landscape. Br. J. Dermatol. Oxford University Press (OUP); 2024;190(2):149–62

Liu J, Xiao Q, Xiao J, Niu C, Li Y, Zhang X, et al. Wnt/β-catenin signalling: function, biological mechanisms, and therapeutic opportunities. Signal Transduct. Target. Ther. Springer Science and Business Media LLC; 2022;7(1):3

Lowe MM, Cohen JN, Moss MI, Clancy S, Adler JP, Yates AE, et al. Tertiary lymphoid structures sustain cutaneous B cell activity in hidradenitis suppurativa. JCI Insight. 2024;9(3)

Mariottoni P, Jiang SW, Prestwood CA, Jain V, Suwanpradid J, Whitley MJ, et al. Single-Cell RNA Sequencing Reveals Cellular and Transcriptional Changes Associated With M1 Macrophage Polarization in Hidradenitis Suppurativa. Front. Med. 2021;8:665873

Moran B, Smith CM, Zaborowski A, Ryan M, Karman J, Dunstan RW, et al. Targeting the NLRP3 inflammasome reduces inflammation in hidradenitis suppurativa skin. Br. J. Dermatol. Br J Dermatol; 2023;189(4):447–58

Navrazhina K, Frew JW, Gilleaudeau P, Sullivan-Whalen M, Garcet S, Krueger JG. Epithelialized tunnels are a source of inflammation in hidradenitis suppurativa. J. Allergy Clin. Immunol. 2021;147(6):2213–24

Nguyen TV, Damiani G, Orenstein LAV, Hamzavi I, Jemec GB. Hidradenitis suppurativa: an update on epidemiology, phenotypes, diagnosis, pathogenesis, comorbidities and quality of life. J. Eur. Acad. Dermatol. Venereol. 2021;35(1):50–61

Pan Y, Lin M-H, Tian X, Cheng H-T, Gridley T, Shen J, et al. gamma-secretase functions through Notch signaling to maintain skin appendages but is not required for their patterning or initial morphogenesis. Dev. Cell. 2004;7(5):731–43

Philippeos C, Telerman SB, Oulès B, Pisco AO, Shaw TJ, Elgueta R, et al. Spatial and single-cell transcriptional profiling identifies functionally distinct human dermal fibroblast subpopulations. J. Invest. Dermatol. 2018;138(4):811–25

Pink AE, Simpson MA, Desai N, Trembath RC, Barker JNW. γ-Secretase mutations in hidradenitis suppurativa: new insights into disease pathogenesis. J. Invest. Dermatol. 2013;133(3):601–7

Reynolds G, Vegh P, Fletcher J, Poyner EFM, Stephenson E, Goh I, et al. Developmental cell programs are co-opted in inflammatory skin disease. Science. 2021;371(6527)

Ring HC, Thorsen J, Saunte DM, Lilje B, Bay L, Riis PT, et al. The Follicular Skin Microbiome in Patients With Hidradenitis Suppurativa and Healthy Controls. JAMA

Dermatol. 2017;153(9):897–905

Riverain-Gillet É, Guet-Revillet H, Jais J-P, Ungeheuer M-N, Duchatelet S, Delage M, et al. The Surface Microbiome of Clinically Unaffected Skinfolds in Hidradenitis Suppurativa: A Cross-Sectional Culture-Based and 16S rRNA Gene Amplicon Sequencing Study in 60 Patients. J. Invest. Dermatol. 2020;140(9):1847–55.e6

Rubtsova K, Rubtsov AV, Thurman JM, Mennona JM, Kappler JW, Marrack P. B cells expressing the transcription factor T-bet drive lupus-like autoimmunity. J. Clin. Invest. 2017;127(4):1392–404

Sabat R, Jemec GBE, Matusiak Ł, Kimball AB, Prens E, Wolk K. Hidradenitis suppurativa. Nat Rev Dis Primers. 2020;6(1):18

Sato Y, Silina K, van den Broek M, Hirahara K, Yanagita M. The roles of tertiary lymphoid structures in chronic diseases. Nat. Rev. Nephrol. Springer Science and Business Media LLC; 2023;19(8):525–37

van Straalen KR, Ma F, Tsou P-S, Plazyo O, Gharaee-Kermani M, Calbet M, et al. Single-cell sequencing reveals Hippo signaling as a driver of fibrosis in hidradenitis suppurativa. J. Clin. Invest. American Society for Clinical Investigation; 2024;134(3)

Sun Q, Broadaway KA, Edmiston SN, Fajgenbaum K, Miller-Fleming T, Westerkam LL, et al. Genetic variants associated with hidradenitis suppurativa. JAMA Dermatol. JAMA Dermatol; 2023;159(9):930–8

Tiri H, Jokelainen J, Timonen M, Tasanen K, Huilaja L. Substantially reduced life expectancy in patients with hidradenitis suppurativa: a Finnish nationwide registry study. Br. J. Dermatol. 2019;180(6):1543–4

Weiss A, Attisano L. The TGFbeta superfamily signaling pathway: TGFbeta superfamily signaling pathway. Wiley Interdiscip. Rev. Dev. Biol. Wiley; 2013;2(1):47–63

Williams SC, Garcet S, Hur H, Miura S, Gonzalez J, Navrazhina K, et al. Gram-negative anaerobes elicit a robust keratinocytes immune response with potential insights into HS pathogenesis. Exp. Dermatol. 2024;33(5):e15087

Yang Y, Gomez N, Infarinato N, Adam RC, Sribour M, Baek I, et al. The pioneer factor SOX9 competes for epigenetic factors to switch stem cell fates. Nat. Cell Biol. Nature Publishing Group; 2023;25(8):1185–95

Yu W-W, Barrett JNP, Tong J, Lin M-J, Marohn M, Devlin JC, et al. Skin immune-mesenchymal interplay within tertiary lymphoid structures promotes autoimmune pathogenesis in hidradenitis suppurativa. Immunity. Elsevier BV; 2024;57(12):2827–42.e5

Zouboulis CC, Benhadou F, Byrd AS, Chandran NS, Giamarellos-Bourboulis EJ, Fabbrocini G, et al. What causes hidradenitis suppurativa ?-15 years after. Exp. Dermatol. 2020;29(12):1154–70

Table 1. Gene signature modules defining keratinocyte states

Cell state	Gene signature module
inflammatory	TNF, IL6, IL1B, CXCL8, CCL2, IL17RA, S100A8, S100A9, TNFAIP3, NFKBIA, IL1B
proliferative	MKI67, TOP2A, KRT6A, KRT16, KRT17, AREG, S100A7
differentiation	IVL, FLG, SPRR1A, DSG1, TGM1
basal	KRT5, KRT14, TP63, ITGA6, COL17A1, LAMC2
hair	KRT75, KRT71, LHX2, HOXC13, SOX9, DCD, AQP5, KRT19, KRT77, KRT18
sebaceous	MUC1, KRT7, FASN, SOAT1
sweat	DCD, AQP5, KRT19, KRT77, KRT18
stress	S100A8, S100A9, SERPINB3, SERPINB4, IFI6, IFITM1, ISG15, CCL20, STAT1, IRF1
HS tunnel	IL36G, IL17A, IL17C, IL17F, CXCL8, IL23A, CXCL1, CXCL2, IL36A, IL36G, IL36RN
notch	NOTCH1, NOTCH2, DLL1, JAG1, JAG2, NCSTN, PSEN1, RBPJ, MAML1, HES1, HEY1
migratory	KRT6, KRT16, KRT17, MMP1, MMP9, MMP10, TMSB4X, VIM, CD44, SNAI2, ZEB1, EGFR, AREG, EREG, HBEGF

Figure and Table Legends:

MAIN

Figure 1. Single-cell landscape of HS skin reveals a novel pathogenic keratinocyte state. **(a)** Skin samples were obtained from 3 donors with severe HS undergoing axillary wide local excision surgery. ScRNAseq (3') and spatial transcriptomics (Visium) were performed on HS skin dissociated cells and 10um

cryosections. *Cell2location*, cell-cell interaction and co-localisation analysis were undertaken to identify the location, identity and function of cells in HS skin. **(b)** Uniform Manifold Approximation and Projection (UMAP) and clustering of 20,003 cells from 3 donors representing 11 skin cell types and 19 cell populations. Each cell is represented by a single point within 2-dimensional space on the UMAP plot, with proximity of points plotted according to global transcriptional similarity. **(c)** Dot plot of established marker genes representative of each cell population. In this representation, the percentage of cells expressing the marker (diameter) and the average log2 normalized expression (color) are shown. **(d)** Violin plots demonstrating gene expression within 7 keratinocyte clusters, of signature functional gene modules (Table 1) related to keratinocyte state characteristics. These included functional modules representing proliferative, basal, differentiated, hair, sweat and sebaceous, as well as HS specific modules with tunnel, inflammatory, migratory and stress response genes. **(e)** Dot plot showing high expression of *S100A7, S100A8, S100A9,* and *S100A12* in the pathogenic keratinocyte state of HS skin. (F) Single-cell trajectory gene analysis using Monocle 3 colored by keratinocyte state. Root node (white) indicates basal keratinocyte with lines indicating trajectory branches (arrows added for clarity) representing cellular decisions. Monocle pseudotime plot, where cells are colored according to differentiation state relative to the cell of origin.

Figure 2. Spatial architecture of keratinocyte states in severe HS. (a) Spatial deconvolution using *cell2location* pipeline of annotated scRNAseq keratinocyte states onto Visium slides, showing localisation of 7 keratinocyte states in severe HS tissue. Predicted cell abundances shown by color gradients per spot in tissue architecture images (H&E in gray).

Figure 3. Cell–cell interactions reveal fibroblast coordination of pathogenic keratinocyte states in severe HS. (a) Circle plot of average intercellular communication probabilities across all significant ligand–receptor pairs between cell populations identified in HS scRNAseq data. Each circle (node) represents a different cell population, with size indicating relative abundance. Lines (edges) connect the cell populations, illustrating communication between them, with the width or thickness indicating the strength and weight of the signaling interaction. **(b)** Circle plot of the total count of ligand–receptor pairs between each cell population identified in HS scRNAseq data. **(c)** Scatter plot showing the dominant senders (sources) and receivers (targets); x-axis and y-axis are respectively the total outgoing or incoming communication probability associated with each cell population. Dot size is proportional to the number of inferred links (both outgoing and incoming) associated with each cell population. Dot colors indicate different cell populations. **(d)** Table indicating the top 20 signalling pathways in HS scRNAseq data, identified by CellChat. **(e)** River plot demonstrating inferred outgoing communication patterns of secreting cells, and the signaling pathways associated with those communication patterns.

Figure 4. Spatial mapping identifies COL6A5+ papillary fibroblast–keratinocyte and SFRP4+ reticular fibroblast–immune niches in HS skin. (a) Spatial cell cluster colocalization analysis for COL6A5+ papillary fibroblasts (F) with all keratinocyte (K) populations using PCC analysis. The bar chart shows pearson correlation coefficients (PCC) of spot normalized cell abundances using the spatial *cell2location* predictions across all spots of Visium samples, with each individual bar

representing a Visium sample (HS donor). **(b)** Spatial cell cluster colocalization analysis for APOD+ inflammatory fibroblasts (F) with all keratinocyte (K) populations using PCC analysis. **(c)** Spatial cell cluster colocalization analysis for SFRP4+ reticular fibroblasts (F) with all keratinocyte (K) populations using PCC analysis. **(d)** Spatial cell cluster colocalization analysis for SFRP4+ reticular fibroblasts and mast cells and macrophages using PCC analysis.

Figure 5. Activated B and plasma cells form spatial niches with fibroblasts and immune cells, indicative of tertiary lymphoid organ development in severe HS. **(a)** Violin plots of gene expression of B cell markers from HS scRNAseq compared to publicly available healthy skin scRNAseq dataset (Ganier et al. 2024) representing an activated B cell phenotype in HS. Each dot is a cell, and the height of dot on the y axis is the normalized expression level. **(b)** Dot plot showing expression of B cell markers in HS versus healthy skin (Ganier et al. 2024) confirming this activated B cell phenotype in HS. **(c)** Immunofluorescent staining was performed on severe HS tissue for CD20, a B cell marker, and CD11c and TBX21, two markers of activated B cells. Co-expression of the markers is marked by white arrows; B cells co-expressing CD20 with CD11c or TBX21 were identified around dermal HS tunnel structures. **(d)** Spatial deconvolution using *cell2location* of annotated scRNAseq plasma/B cells onto Visium slides, confirmed their localisation in severe HS tissue. Predicted cell abundances shown by color gradients per spot in tissue architecture images (H&E in gray)**.** **(e)** Gene expression of IGHA1, IGHM, IGHG1, representing antibody production by B/plasma cells in Visium data is detected in most HS samples throughout the dermis, with color gradient indicating gene expression level. **(f)** Dot plot of genes representing plasma cell markers (SDC1, PRDM1, JCHAIN) and

antibody production (IGHA1, IGHM, IGHG1) in HS scRNAseq dataset confirming this antibody production mainly by plasma cells but also by B cells in HS skin. **(g)** Spatial cell cluster colocalization analysis for plasma/B cells with all fibroblast populations, immune cells and endothelial cells using PCC analysis. The bar chart shows PCC of spot normalized cell abundances using the spatial *cell2location* predictions across all spots of Visium samples, with each individual bar representing a Visium sample (HS donor). **(h)** Spatial cell cluster colocalization analysis for APOD+ fibroblasts with other fibroblast subpopulations, endothelial cells, pericytes and langerhans cells using PCC analysis. **(i)** Spatial cell cluster colocalization analysis for Langerhans cells with fibroblast subpopulations, endothelial cells and pericytes using PCC analysis.

Table 1. Gene signature modules defining keratinocyte states. Keratinocytes state characteristics and associated gene signature modules based upon well-known markers established within the literature.

SUPPLEMENTAL

Supplementary Figure 1. Metadata and quality control metrics of scRNAseq and spatial transcriptomics in HS samples. (a) Relevant metadata from 3 donors with severe HS. **(b)** Violin plots of key quality control parameters related to scRNAseq data from 3 donors with severe HS, showing frequency distribution of log1p-transformed unique molecular identifier (UMI) counts (left panel), gene counts (middle panel) and percentage of mitochondrial genes (right panel). **(c)** Violin plots of quality control parameters related to Visium data across all samples, showing

frequency distribution of UMI counts (log1p-transformed) per spot (upper panel), gene counts per spot (middle panel) and percentage of mitochondrial genes per spot (lower panel). **(d)** Spatial distribution of UMI counts (nCount_spatial) across all HS tissue sections processed with the 10X Visium protocol.

Supplementary Figure 2. Spatial mapping of keratinocyte states in healthy human skin and comparison of immune and endothelial cellular populations in HS, Eczema, Psoriasis, and Healthy Skin. (a) Spatial deconvolution of annotated scRNAseq keratinocyte states onto Visium slides of publicly available healthy skin scRNAseq dataset (Ganier et al. 2024) using *cell2location*, showing localisation of 7 keratinocyte states in healthy skin tissue. Predicted cell abundances shown by color gradients per spot in tissue architecture images (H&E in gray). Dividing K are seen scattered within basal interfollicular epidermis (IFE). Basal K are identified in the basal layer of IFE. Basal/spinous K were located in between basal and spinous layers of the IFE and throughout the pilosebaceous unit (PSU). Transitional remodeling K were deconvoluted throughout the IFE layers, except for the granular layer and extending into the upper PSU. Immunobarrier K were spatially consistent with the most differentiated and granular layer of the IFE. Hair and sweat glandular keratinocytes were seen in the lower PSU. Migratory S100+ K / sebocytes were identified within sebaceous glands of the PSU. **(b)** Analysis of proportions of cellular populations in HS scRNAseq data compared to lesional eczema, lesional psoriasis and healthy skin from (Reynolds et al. 2021). Stacked bar chart showing relative proportions of immune cell populations in scRNAseq in those datasets. T cells are proportionally higher in psoriasis and eczema skin, whereas plasma cells and mast cells are proportionally higher in HS skin. **(c)** Endothelial cells from lesional eczema

skin, HS skin, psoriasis skin and healthy skin were examined for presence or absence of ACKR1 expression on a per cell basis. Proportions of ACKR1-expressing cells against ACKR1-negative cells from each dataset are shown in a stacked bar chart.

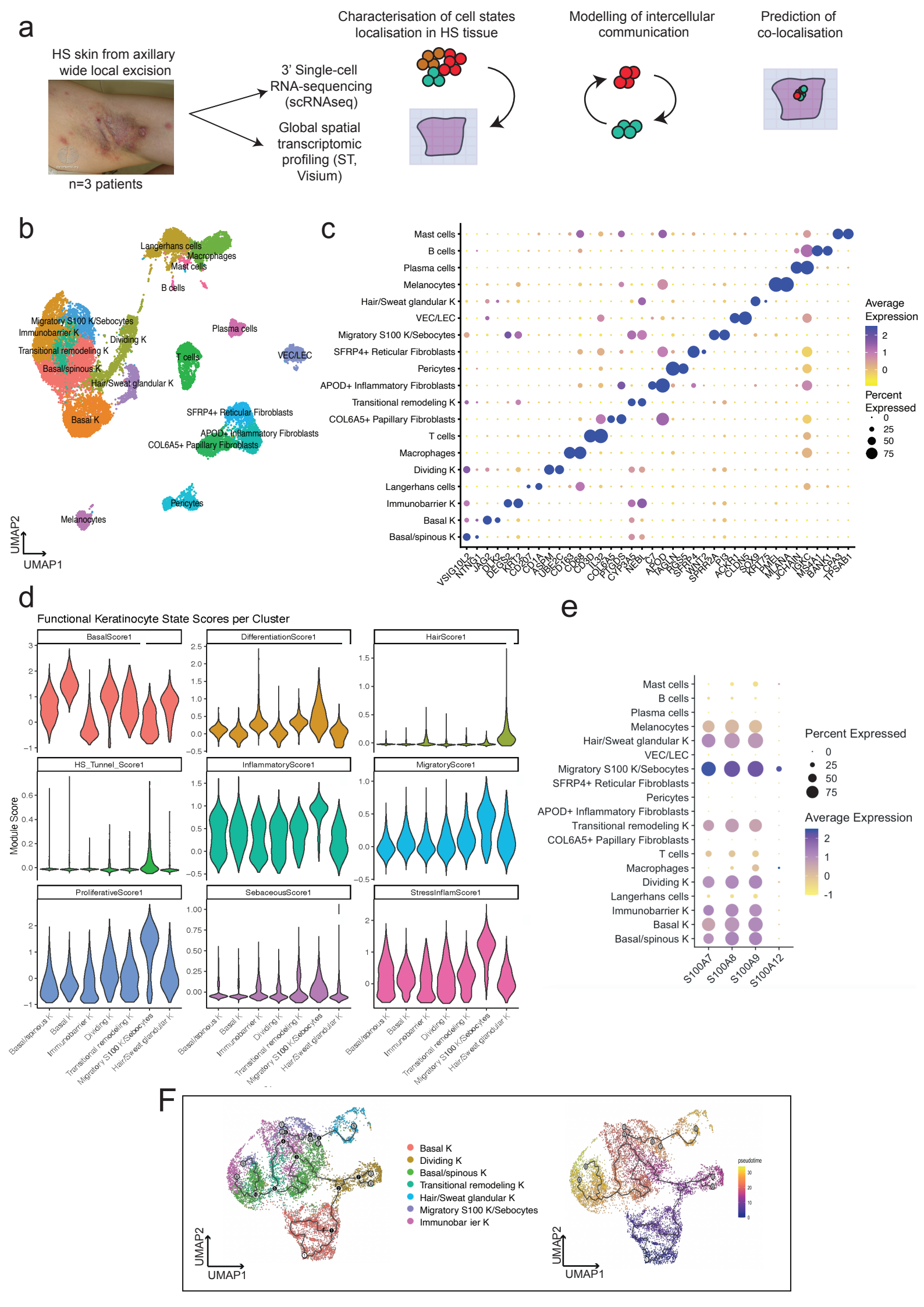
a
HS skin from axillary wide local excision
n=3 patients
3' Single-cell RNA-sequencing (scRNAseq)
Global spatial transcriptomic profiling (ST, Visium)
Characterisation of cell states localisation in HS tissue
Modelling of intercellular communication
Prediction of co-localisation
b
Langerhans cells
Macrophages
Mast cells
B cells
Migratory S100 K/Sebocytes
Immunobarrier K
Dividing K
Transitional remodeling K
Basal/spinous K
Hair/Sweat glandular K
Basal K
Plasma cells
T cells
VEC/LEC
SFRP4+ Reticular Fibroblasts
APOD+ Inflammatory Fibroblasts
COL6A5+ Papillary Fibroblasts
Pericytes
Melanocytes
UMAP2
UMAP1
c
Mast cells
B cells
Plasma cells
Melanocytes
Hair/Sweat glandular K
VEC/LEC
Migratory S100 K/Sebocytes
SFRP4+ Reticular Fibroblasts
Pericytes
APOD+ Inflammatory Fibroblasts
Transitional remodeling K
COL6A5+ Papillary Fibroblasts
T cells
Macrophages
Dividing K
Langerhans cells
Immunobarrier K
Basal K
Basal/spinous K
Average Expression
Percent Expressed
d
Functional Keratinocyte State Scores per Cluster
BasalScore1
DifferentiationScore1
HairScore1
HS_Tunnel_Score1
InflammatoryScore1
MigratoryScore1
ProliferativeScore1
SebaceousScore1
StressInflamScore1
Module Score
e
S100A7
S100A8
S100A9
S100A12
Percent Expressed
Average Expression
F
Basal K
Dividing K
Basal/spinous K
Transitional remodeling K
Hair/Sweat glandular K
Migratory S100 K/Sebocytes
Immunobar ier K
pseudotime
UMAP2
UMAP1

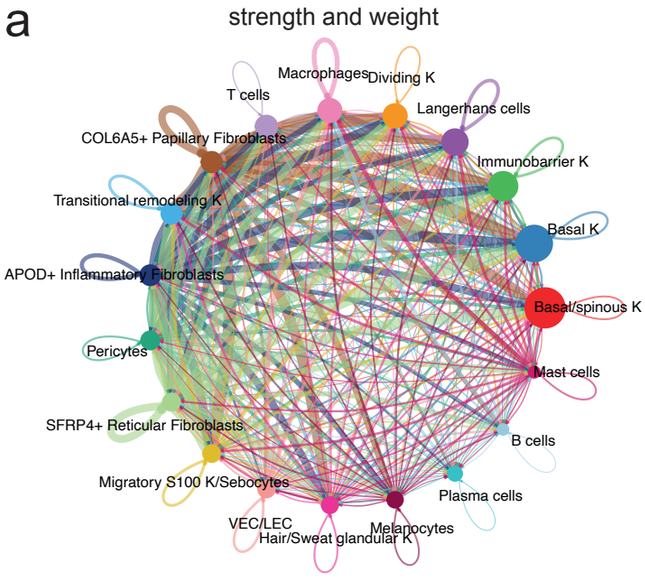

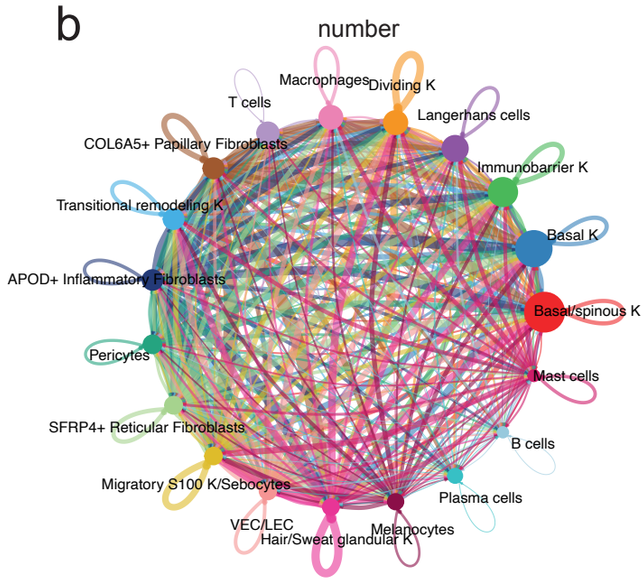

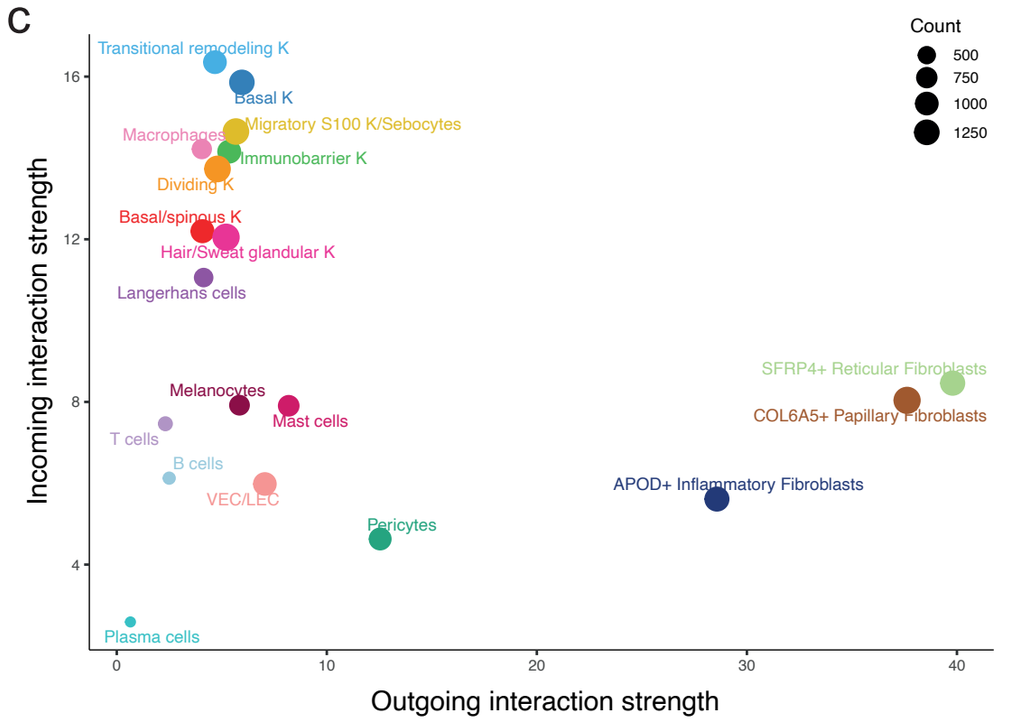

d

Top 20 signalling pathways

1	COLLAGEN
2	LAMININ
3	DESMOSOME
4	CD99
5	MIF
6	MHC-II
7	FN1
8	APP
9	MK
10	THBS
11	CXCL
12	EGF
13	NOTCH
14	TENASCIN
15	CDH
16	PTN
17	CD46
18	VISFATIN
19	ANGPTL
20	CLEC

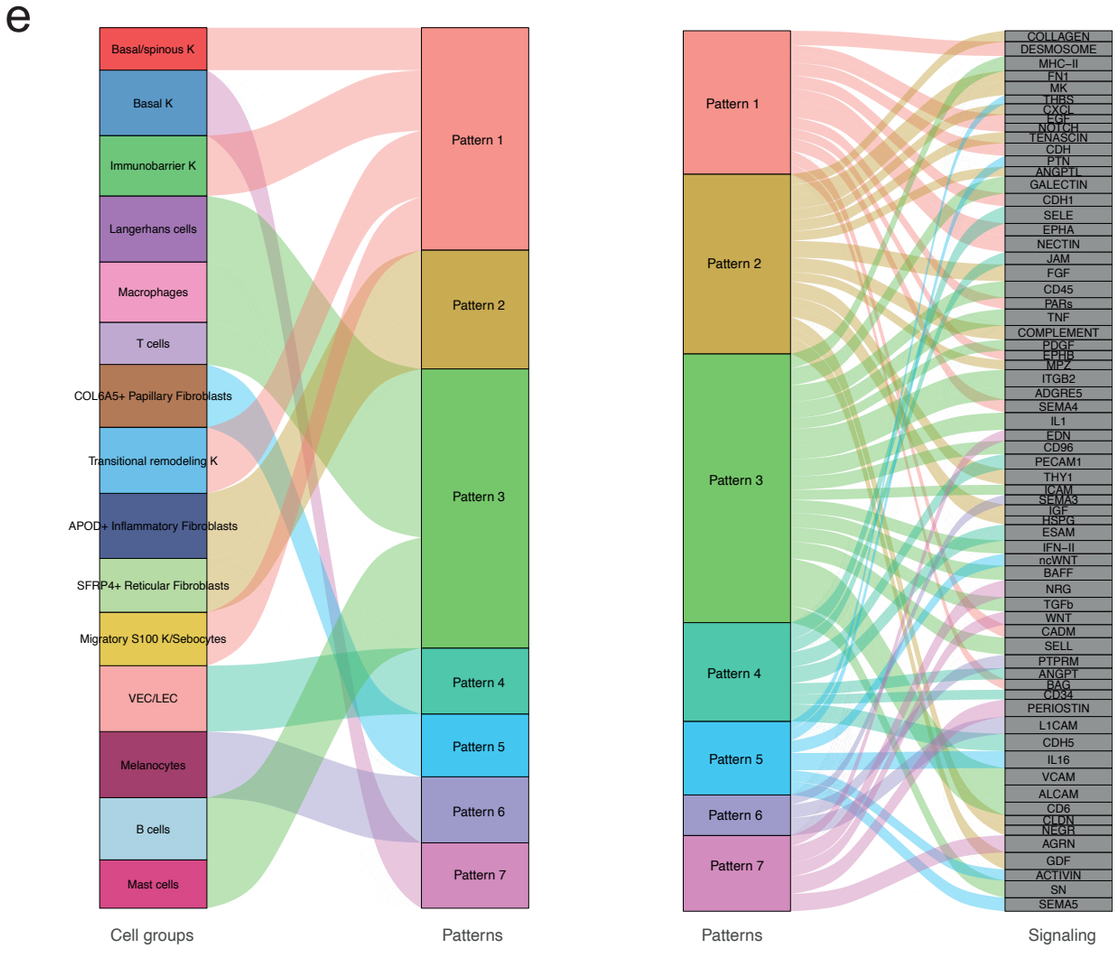

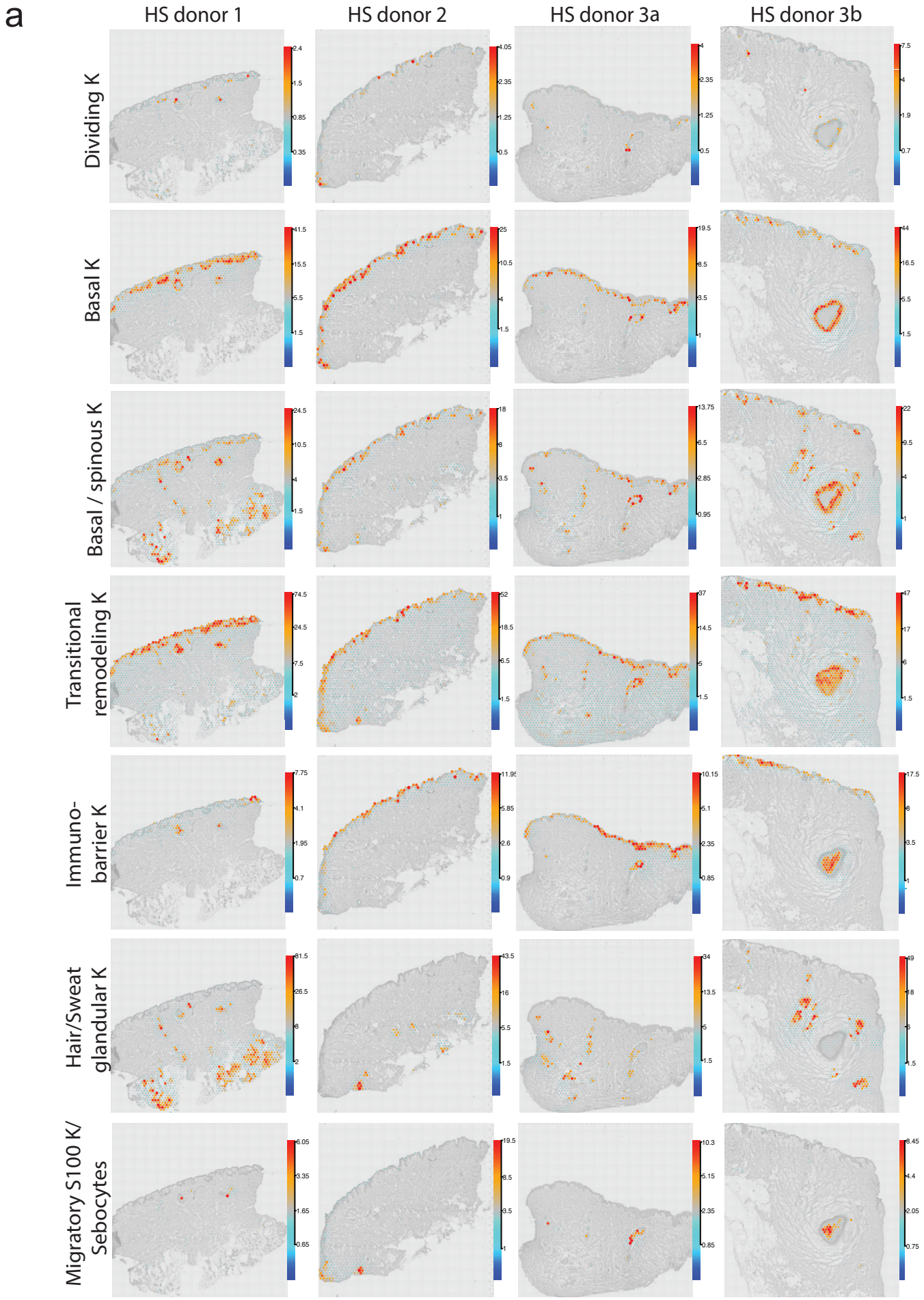
a
HS donor 1
HS donor 2
HS donor 3a
HS donor 3b
Dividing K
Basal K
Basal / spinous K
Transitional remodeling K
Immuno-barrier K
Hair/Sweat glandular K
Migratory S100 K/ Sebocytes

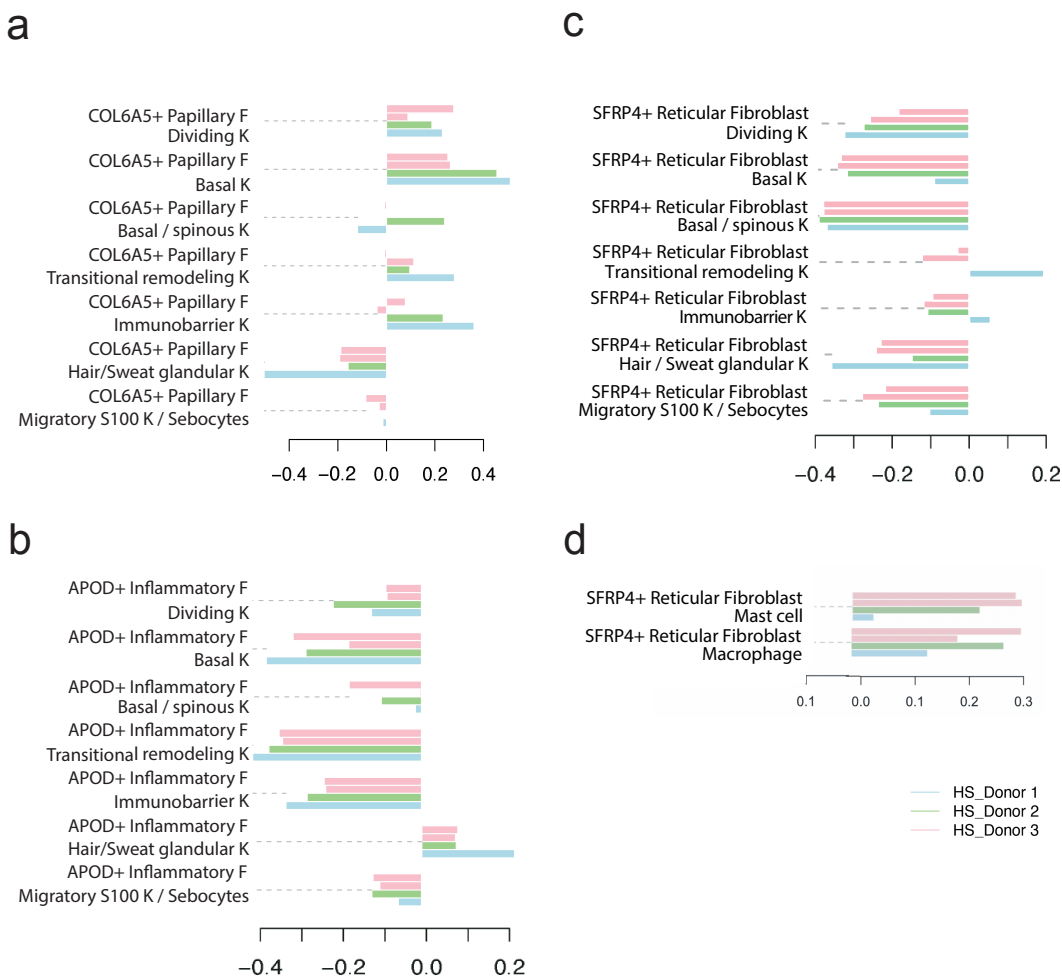
a
COL6A5+ Papillary F
Dividing K
COL6A5+ Papillary F
Basal K
COL6A5+ Papillary F
Basal / spinous K
COL6A5+ Papillary F
Transitional remodeling K
COL6A5+ Papillary F
Immunobarrier K
COL6A5+ Papillary F
Hair/Sweat glandular K
COL6A5+ Papillary F
Migratory S100 K / Sebocytes
−0.4 −0.2 0.0 0.2 0.4
c
SFRP4+ Reticular Fibroblast
Dividing K
SFRP4+ Reticular Fibroblast
Basal K
SFRP4+ Reticular Fibroblast
Basal / spinous K
SFRP4+ Reticular Fibroblast
Transitional remodeling K
SFRP4+ Reticular Fibroblast
Immunobarrier K
SFRP4+ Reticular Fibroblast
Hair / Sweat glandular K
SFRP4+ Reticular Fibroblast
Migratory S100 K / Sebocytes
−0.4 −0.2 0.0 0.2
b
APOD+ Inflammatory F
Dividing K
APOD+ Inflammatory F
Basal K
APOD+ Inflammatory F
Basal / spinous K
APOD+ Inflammatory F
Transitional remodeling K
APOD+ Inflammatory F
Immunobarrier K
APOD+ Inflammatory F
Hair/Sweat glandular K
APOD+ Inflammatory F
Migratory S100 K / Sebocytes
−0.4 −0.2 0.0 0.2
d
SFRP4+ Reticular Fibroblast
Mast cell
SFRP4+ Reticular Fibroblast
Macrophage
0.1 0.0 0.1 0.2 0.3
HS_Donor 1
HS_Donor 2
HS_Donor 3

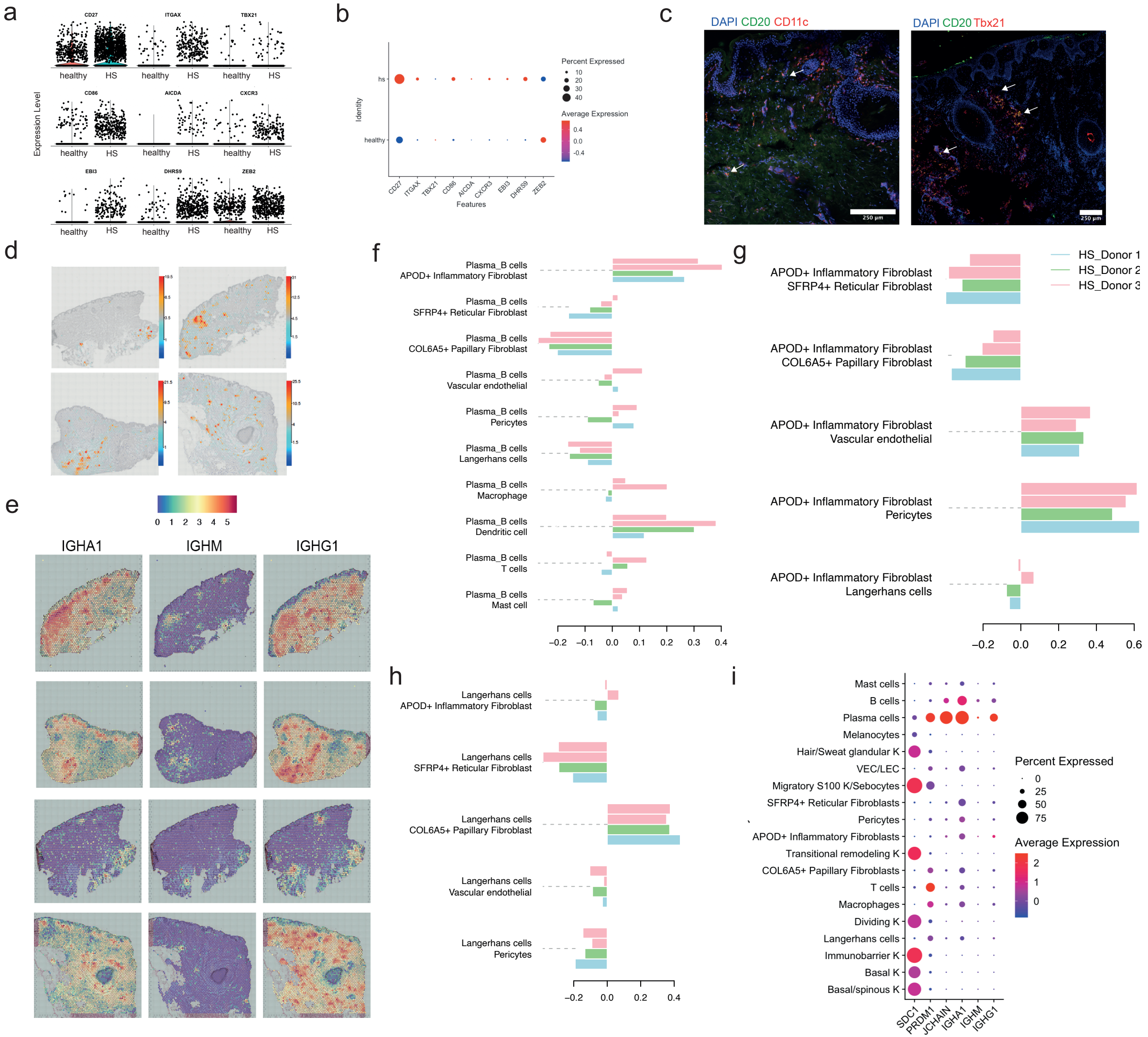
a
CD27
ITGAX
TBX21
CD86
AICDA
CXCR3
EBI3
DHRS9
ZEB2
healthy
HS
Expression Level
b
Percent Expressed
10
20
30
40
Average Expression
0.4
0.0
-0.4
hs
healthy
Identity
Features
c
DAPI CD20 CD11c
DAPI CD20 Tbx21
250 µm
d
e
IGHA1
IGHM
IGHG1
0 1 2 3 4 5
f
Plasma_B cells
APOD+ Inflammatory Fibroblast
SFRP4+ Reticular Fibroblast
COL6A5+ Papillary Fibroblast
Vascular endothelial
Pericytes
Langerhans cells
Macrophage
Dendritic cell
T cells
Mast cell
−0.2 −0.1 0.0 0.1 0.2 0.3 0.4
g
HS_Donor 1
HS_Donor 2
HS_Donor 3
APOD+ Inflammatory Fibroblast
SFRP4+ Reticular Fibroblast
COL6A5+ Papillary Fibroblast
Vascular endothelial
Pericytes
Langerhans cells
−0.2 0.0 0.2 0.4 0.6
h
Langerhans cells
APOD+ Inflammatory Fibroblast
SFRP4+ Reticular Fibroblast
COL6A5+ Papillary Fibroblast
Vascular endothelial
Pericytes
−0.2 0.0 0.2 0.4
i
Mast cells
B cells
Plasma cells
Melanocytes
Hair/Sweat glandular K
VEC/LEC
Migratory S100 K/Sebocytes
SFRP4+ Reticular Fibroblasts
Pericytes
APOD+ Inflammatory Fibroblasts
Transitional remodeling K
COL6A5+ Papillary Fibroblasts
T cells
Macrophages
Dividing K
Langerhans cells
Immunobarrier K
Basal K
Basal/spinous K
SDC1
PRDM1
JCHAIN
IGHA1
IGHM
IGHG1
Percent Expressed
0
25
50
75
Average Expression
2
1
0